*Inorg. Chem.* **2008**, *47*, 7396−7404

# 1D Molecular Ladder of the Ionic Complex of Terbium-4-Sebacoylbis(1-phenyl-3-methyl-5-pyrazolonate) and Sodium Dibenzo-18-Crown-6: Synthesis, Crystal Structure, and Photophysical Properties

**P.N. Remya,[†] S. Biju,[†] M. L. P. Reddy,*[,†] Alan H. Cowley,[‡] and Michael Findlater[‡]**

*Chemical Sciences and Technology Division, National Institute for Interdisciplinary Science & Technology (NIIST), Thiruvananthapuram-695 019, India, and Department of Chemistry and Biochemistry, The University of Texas at Austin, 1 University Station A5300, Austin, Texas 78712*

Received April 5, 2008

On the basis of the novel heterocyclic $\beta$-diketone, 4-sebacoylbis(1-phenyl-3-methyl-5-pyrazolone ($H_2$SbBP), three new lanthanide complexes $Tb_2(SbBP)_3(H_2O)_2$ (**1**), $Gd_2(SbBP)_3(H_2O)_2$ (**2**), and [Tb(SbBP)$_2$] [Na(DB18C6)$H_2O$] (**3**) have been synthesized and characterized by various spectroscopic techniques. The single-crystal X-ray diffraction analysis of **3** reveals that the complex crystallizes in the monoclinic space group *C*2/*c* with $a = 25.300(6)$ Å, $b = 19.204(7)$ Å, $c = 15.391(3)$ Å, $\beta = 93.17(3)°$, and $V = 7466(4)$ Å$^3$. The crystal structure of **3** is heterodinuclear and features a $Tb^{3+}$ center surrounded by two tetradentate bispyrazolone ligands in a somewhat distorted square-antiprismatic geometry. The $Na^+$ coordination environment is distorted hexagonal pyramidal and involves six oxygen atoms furnished by DB18C6 and one oxygen atom from a water molecule. The X-ray diffraction study of **3** also revealed an interesting 1D molecular ladder structure based on C−H/$\pi$, intra- and intermolecular hydrogen-bonding interactions. The photophysical properties of **1** and **3** in solid state have been investigated, and the quantum yields and $^5D_4$ lifetimes were found to be 4.82 ± 0.01% and 18.13 ± 0.82% and 1.11 ± 0.01 and 2.82 ± 0.02 ms, respectively.

## Introduction

The design and the synthesis of organolanthanide complexes continues to receive increasing attention because of their potential applications of such complexes in a wide range of photonic applications that includes tunable lasers, amplifiers for optical communications, components of emitting materials in multilayer organic light-emitting diodes, and luminescent probes for analytes.[1] The $\beta$-diketone ligand class represents one of the important antennae for facilitating efficient energy transfer from to $Eu^{3+}$ and $Tb^{3+}$ ions, thus generating high harvest emissions.[2,3] Moreover, $\beta$-diketones have the additional advantage of a negatively charged binding site that results in the formation of neutral, 3:1 ligand/lanthanide luminescent complexes.[4–6] Furthermore, these ligands exhibit strong absorption over a large wavelength

* To whom correspondence should be addressed. E-mail: mlpreddy@yahoo.co.uk.
[†] National Institute for Interdisciplinary Science & Technology (NIIST).
[‡] The University of Texas at Austin.

(1) (a) de Sa, G. F.; Malta, O. L.; de Mello Donega, C.; Simas, A. M.; Longo, R. L.; Santa-Cruz, P. A.; da Silva, E. F., Jr *Coord. Chem. Rev.* **2000**, *196*, 165–195. (b) Piguet, C.; Bünzli, J.-C. G. *Chem. Soc. Rev.* **2005**, *34*, 1048–1077. (c) Kido, J.; Okamoto, Y. *Chem. Rev.* **2002**, *102*, 2357–2368. (d) de Bettencourt-Dias, A. *Dalton Trans.* **2007**, 2229–2241. (e) Kuriki, K.; Koike, Y.; Okamoto, Y. *Chem. Rev.* **2002**, *102*, 2347–2356.

(2) (a) Binnemans, K. *Handbook on the Physics and Chemistry of Rare Earths*, Elsevier: Amsterdam, The Netherlands, 2005; Chapter 225, Vol. *35*, pp 107−272. (b) Sinha, S. P. *Complexes of the Rare Earth*; Pergamon: London, 1966.

(3) (a) Wang, J.; Wang, R.; Yang, J.; Zheng, Z.; Carducci, M. D.; Cayon, T.; Peyghambarian, N.; Jabbour, G. E. *J. Am. Chem. Soc.* **2001**, *123*, 6179–6180. (b) Bassett, A. P.; Magennis, S. W.; Glover, P. B.; Lewis, D. J.; Spencer, N.; Parsons, S.; Williams, R. M.; De Cola, L.; Pikramenou, Z. *J. Am. Chem. Soc.* **2004**, *126*, 9413–9424.

(4) (a) Weissman, S. I. *J. Chem. Phys.* **1942**, *10*, 214. (b) Sun, L.; Yu, J.; Zheng, G.; Zhang, H.; Meng, Q.; Peng, C.; liu, F.; Yu, Y. *Eur. J. Inorg. Chem.* **2006**, 3962–3973.

(5) (a) Yu, J.; Zhang, L. Z. H.; Zheng, Y.; Li, H.; Peng, R. D. Z.; Li, Z. *Inorg. Chem.* **2005**, *44*, 1611–1618. (b) Fratini, A.; Richards, G.; Larder, E.; Swavey, S. *Inorg. Chem.* **2008**, *47*, 1030–1036.

(6) (a) Hasegawa, Y.; Yamamuro, M.; Wada, Y.; Kanehisa, N.; Kai, Y.; Yanagida, S. *J. Phys. Chem. A.* **2003**, *107*, 1697–1702. (b) Eliseeva, S. V.; Ryazanov, M.; Gumy, F.; Troyanov, S. I.; Lepenev, L. S.; Bunzil, J. C. G.; Kuzmina, N. P. *Eur. J. Inorg. Chem.* **2006**, 4809–4820.



10.1021/ic800615y CCC: $40.75 
Published on Web 07/24/2008

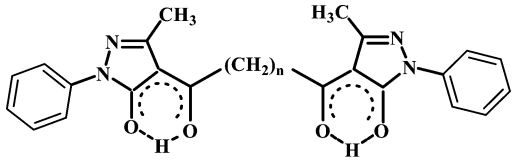


**Figure 1.** Molecular structure of 4-acylbis(pyrazolones).

range for the $\pi-\pi^*$ transition and can therefore sensitize the lanthanide luminescence effectively.[4–6] As a consequence, a significant number of lanthanide tris($\beta$-diketonates) that also feature coordinated nitrogen ligands such as 1,10-phenanthroline,[7] 4,7-disubstituted-1,10-phenanthrolines, 2,2′-bipyridine,[8] 4,4′-disubstituted-2,2′-bipyridines,[8] and 2,2′:6′,6″-terpyridine[9] has been reported to serve as efficient light-conversion molecular devices.

It has been reported recently that heterocyclic $\beta$-diketonates such as 4-acyl-5-pyrazolones[10,11] and 3-phenyl-4-benzoyl-5-isoxazolones[12] can also be successfully employed as sensitizers for $Eu^{3+}$ and $Tb^{3+}$. Moreover, the terbium complexes that are supported by the pyrazolone-based ligands 1-phenyl-3-methyl-4-isobutyryl-5-pyrazolone and 1-phenyl-3-methyl-4-(2-ethylbutyryl)-5-pyrazolone[13] are reported to emit characteristic $Tb^{3+}$ photoluminescence with high quantum yields. However, another novel class of 4-acylbis(pyrazolones), in which two 1-phenyl-3-methyl-4-acyl-5-pyrazolone subunits are linked by a polymethylene chain of various lengths $-(CH_2)_n-$ ($n = 0-8$, 10, 20) have not been employed as sensitizers for lanthanides even though they are well-known as potential complexing agents for the lanthanides (Figure 1).[14] Furthermore, the 4-acyl-5-pyrazolone derivatives that possess two $\beta$-diketone donor sites on both sides of the polymethylene chain are expected to result in specific complexation depending on the polymethylene chain length. Herein, we report the synthesis, crystal structure and photophysical properties of new terbium(III) complexes of 1-phenyl-3-methyl-4-sebacoyl-5-pyrazolone ($H_2$SbBP) and dibenzo-18-crown-6 (DB18C6).

## Experimental Section

**Materials and Instrumentation.** The commercially available chemicals terbium(III) nitrate hexahydrate (99.9%, Acros Organics), gadolinium(III) nitrate hexahydrate (99.9%, Acros Organics), and dibenzo-18-crown-6 (98%, Aldrich) were used without further purification. All of the other chemicals used were of analytical reagent grade.

Elemental analyses were performed with a PerkinElmer Series 2 Elemental Analyzer 2400. A Nicolet FTIR 560 Magna Spectrometer using KBr (neat) was used to obtain the IR spectral data, and a Bruker 300 MHz NMR spectrometer was used for the acquisition of $^1$H NMR spectral data in $CDCl_3$ solution. The diffuse reflectance spectra of the new lanthanide complexes and the standard phosphor were recorded on a Shimadzu, UV-2450 UV−vis spectrophotometer using $BaSO_4$ as a reference. The absorbances of the ligands and the corresponding complexes were measured in $CHCl_3$ solution on a UV−vis spectrophotometer (Shimadzu, UV-2450). The photoluminescence (PL) spectra were recorded using a Spex-Fluorolog DM3000F spectrofluorometer with a double grating, 0.22m Spex 1680 monochromator, and a 450 W xenon lamp as the excitation source (front-face mode). The excitation and emission spectra of the complexes were corrected for instrumental function. The lifetime measurements were carried out at room temperature using a Spex 1934 D phosphorimeter.

The overall quantum yields ($\Phi_{overall}$) were measured at room temperature using the technique for powdered samples described by Bril et al.,[15] and the following expression:

$$\Phi_{overall} = \left(\frac{1-r_{st}}{1-r_x}\right)\left(\frac{A_x}{A_{st}}\right)\Phi_{st} \qquad (1)$$

where $r_{st}$ and $r_x$ represent the diffuse reflectance (with respect to a fixed wavelength) of the complexes and of the standard phosphor, respectively, and $\Phi_{st}$ is the quantum yield of the standard phosphor. The terms $A_x$ and $A_{st}$ represent the areas under the complex and the standard emission spectra, respectively. To acquire absolute intensity values, $BaSO_4$ was used as a reflecting standard. The standard phosphor used was sodium salicylate (Merck), the emission spectrum of which comprises an intense broadband with a maximum at approximately 425 nm, and a constant $\Phi$ value (60%) for excitation wavelengths between 220 and 380 nm. Three measurements were carried out for each sample, and the reported $\Phi_{overall}$ value corresponds to the arithmetic mean value of the three values. The errors in the quantum yield values associated with this technique were estimated to be $\pm 10\%$.[16]

The single-crystal X-ray diffraction data for **3** were collected at 153 K on a Nonius Kappa CCD diffractometer equipped with an Oxford Cryostream low-temperature device and a graphite-monochromated Mo K$\alpha$ radiation source ($\lambda = 0.71073$ Å). Corrections were applied for Lorentz and polarization effects. The structure was solved by direct methods[17] and refined by full-matrix least-squares cycles on $F^2$. All non-hydrogen atoms were allowed anisotropic thermal motion, and the hydrogen atoms were placed in fixed, calculated positions using a riding model (C−H 0.96 Å).

(7) Watson, W. H.; Williams, R. J.; Stemple, N. R. *J. Inorg. Chem.* **1972**, *34*, 501–508.
(8) Bellusci, A.; Barberio, G.; Crispini, A.; Ghedini, M.; La Deda, M.; Pucci, D. *Inorg. Chem.* **2005**, *44*, 1818–1825.
(9) Chen, Y. X.; bretonniere, Y.; Pecaut, J.; Imbert, D.; Bunzil, J.-C.; Mazzanti, M. *Inorg. Chem.* **2007**, *46*, 625–637.
(10) (a) Li, S.; Mei, S.; Fuyou, L.; Zhang, D.; Li, X.; Shi, E.; Yi, T.; Du, Y.; Huang, C. *Inorg. Chem.* **2006**, *45*, 6188–6197. (b) Xin, H.; Shi, M.; Gao, X. C.; Huang, Y. Y.; Gong, Z. L.; Nie, D. B.; Cao, H.; Bian, Z. Q.; Li, F. Y.; Huang, C. H. *J. Phys. Chem. B* **2004**, *108*, 10796–10800.
(11) Shi, M.; Li, F.; Yi, T.; Zhang, D.; Hu, H.; Huang, C. *Inorg. Chem.* **2005**, *44*, 8929–8936.
(12) (a) Biju, S.; Ambili Raj, D. B.; Reddy, M. L. P.; Kariuki, B. M. *Inorg. Chem.* **2006**, *45*, 10651–10660. (b) Pavithran, R.; Saleesh Kumar, N. S.; Biju, S.; Reddy, M. L. P.; Freire, R. O. *Inorg. Chem.* **2006**, *45*, 2184–2192. (c) Pavithran, R.; Reddy, M. L.P.; Alves, S., Jr.; Freire, R. O.; Rocha, G. B.; Lima, P. P. *Eur. J. Inorg. Chem.* **2005**, *20*, 4129–4137. (d) Biju, S.; Reddy, M. L. P.; Freire, R. O. *Inorg. Chem. Commun.* **2007**, *10*, 393–396.
(13) (a) Xin, H.; Li, F. Y.; Shi, M.; Bian, Z. Q.; Huang, C. H. *J. Am. Chem. Soc.* **2003**, *125*, 7166–7167. (b) Xin, H.; Shi, M.; Zhang, X. M.; Li, F. Y.; Bian, Z. Q.; Ibrahim, K.; Liu, F. Q.; Huang, C. H. *Chem. Mater.* **2003**, *15*, 3728–3733.
(14) (a) Pavithran, R.; Reddy, M. L. P. *Anal. Chim. Acta* **2005**, *536*, 219–226. (b) Reddy, M. L. P.; Sahu, S. K.; Chakravortty, V. *Solvent Extr. Ion Exch.* **2000**, *18*, 1135–1153.
(15) Bril, A.; De Jager-Veenis, A. W. *J. Electrochem. Soc.* **1976**, *123*, 396–398.
(16) (a) Mello Donega, C. D.; Junior, S. A.; de Sa, G. F. *Chem. Commun.* **1996**, *11*, 1199–1200. (b) Carlos, L. D.; Mello Donega, C. D.; Albuquerque, R. Q.; Junior, S. A.; Menezes, J. F. S.; Malta, O. L. *Mol. Phys.* **2003**, *101*, 1037–1045.
(17) (a) Sheldrick, G. M., *SHELL-PC, version 5*; Siemens Analytical X-ray Instruments. Inc.: Madison, WI, U.S.A., 1994.

**Scheme 1.** Synthesis of $H_2SbBP$

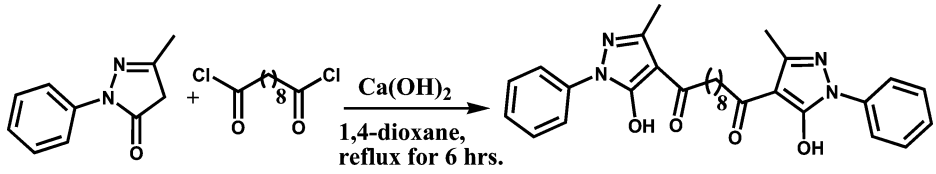


**Scheme 2.** Synthesis Routes to **1** and **2**

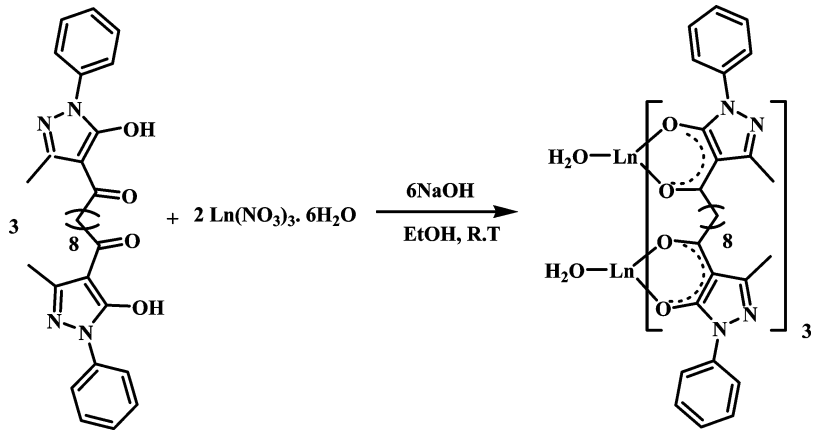


**Synthesis of 4-sebacoylbis(1-phenyl-3-methyl-5-pyrazolone).** 4-Sebacoylbis(1-phenyl-3-methyl-5-pyrazolone) was synthesized by acylation of 1-phenyl-3-methyl-5-pyrazolone with sebacoyl chloride (Scheme 1).[14] Product was recrystallized from a chloroform/hexane mixture and characterized by elemental analysis along with FTIR and $^1$H NMR spectroscopic data.

Elemental analysis: Calcd for $C_{30}H_{34}O_4N_4$: (514.62) C, 70.03; H, 6.61; N, 10.89. Found: C, 69.48; H, 6.51; N, 10.67%; $^1$H NMR data($CDCl_3$/TMS): $\delta$ 7.81−7.84, 7.42−7.47, 7.28−7.30 (m, 10H, Ph); 2.71−2.76 (t, 4H, $(CH_2)_2$); 2.48 (s, 6H, $CH_3$); 1.73−1.77 (m, 4H, $(CH_2)_2$); 1.39 (m, 8H, $(CH_2)_4$); IR (KBr) data ($\nu$ cm$^{-1}$): 3430 (br, OH); 1620 (s, C═O); 1593 (s, phenyl C═C); 1553 (s, pyrazolone ring).

**Syntheses of $Tb_2(SbBP)_3(H_2O)_2$ (1) and $Gd_2(SbBP)_3(H_2O)_2$ (2).** [Ln = $Tb^{3+}$ (**1**), $Gd^{3+}$(**2**)]. Sodium hydroxide (0.6 mmol) was added to an ethanolic solution of $H_2SbBP$ (0.3 mmol), and the mixture was stirred for 5 min. A saturated ethanolic solution of $Ln(NO_3)_3\cdot 6H_2O$ (0.2 mmol) was added dropwise, and the reaction mixture was stirred for 10 h at ambient temperature. Distilled water was then added in sufficient quantity to cause precipitation, and the resulting precipitate was separated by filtration, and then washed several times with distilled water. After drying, the product was purified by recrystallization from an acetone−water mixture (Scheme 2). Unfortunately, all efforts to grow single crystals of **1** and **2** were unsuccessful.

**$Tb_2(SbBP)_3(H_2O)_2$ (1).** Elemental analysis: Calcd for $C_{90}H_{100}N_{12}O_{14}Tb_2$ (**1**) (1890.6): C, 57.14; H, 5.33; N, 8.89. Found: C, 57.75; H, 5.89; N, 8.21. IR (KBr) $\nu_{max}$: 3390, 1610, 1591, 1434, 1366, 1013, 755 cm$^{-1}$. MS(FAB) $m/z$ = 1855 ($M^+$ - $2H_2O$).

**$Gd_2(SbBP)_3(H_2O)_2$ (2).** Elemental analysis: Calcd for $C_{90}H_{100}N_{12}O_{14}Gd_2$ (**2**) (1888.33): C, 52.26; H, 3.82; N, 10.45. Found: C, 52.36; H, 3.78; N, 10.78. IR (KBr) $\nu_{max}$: 3369, 1618, 1594, 1488, 1371, 1002, 758 cm$^{-1}$. MS (FAB) $m/z$ = 1852 ($M^+$ - $2H_2O$).

**Synthesis of [Na(DB18C6)$H_2O$] [Tb($SbBP)_2$] (3).** An aqueous solution of $Tb(NO_3)_3\cdot 6H_2O$ (0.5 mol) was added to a mixture of $H_2SbBP$ (2 mmol) in ethanol and DB18C6 (1.0 mmol) in the presence of NaOH (4 mmol). The reaction mixture was stirred at room temperature for 10 h (Scheme 3). The walls of the reaction vessel show green luminescence when exposed to portable UV torch. A crop of crystals were formed after ~1 week. The crystalline product was filtered, washed with ethanol, water, and then ethanol. After drying, the product was stored in a desiccator. Elemental analysis: Calcd for $C_{80}H_{88}N_8O_{15}TbNa$ (1583.49): C, 60.60; H, 5.72; N, 7.07. Found: C, 60.26; H, 5.82; N, 7.45. IR (KBr) $\nu_{max}$: 3468, 1613, 1594, 1499, 1384, 1253, 1064, 1031, 848, 760 cm$^{-1}$.

**$Gd(DB18C6)_2(NO_3)_3(H_2O)_2$ (4).** An aqueous solution of $Gd(NO_3)_3\cdot 6H_2O$ (0.5 mol) was added to an ethanolic solution of DB18C6 (1.0 mmol). Then the reaction mixture was stirred at room temperature for 10 h. The precipitate formed after 48 h was filtered, washed with ethanol, water, and then ethanol. After drying, the product was stored in a desiccator. Elemental analysis: Calcd for $C_{40}H_{50}O_{13}Gd$ (**4**) (1100.25): C, 43.67; H, 4.76;N, 3.82 Found: C, 43.36; H, 4.78; N, 3.12; IR (KBr) $\nu_{max}$: 3369, 1218, 1194, 1118, 1012, 754 cm$^{-1}$. MS (FAB) $m/z$ = 1101 ($M^+$ - $2H_2O$).

## Results and Discussion

**Structural Characterization of $Ln^{3+}$ Complexes.** The synthetic procedures for the lanthanide complexes **1**−**2** and **3** are summarized in Schemes 2 and 3, respectively. The elemental analysis and FAB-MS mass spectral data for **1** and **2** indicate that $Ln^{3+}$ ion has reacted with $H_2SbBP$ in a metal-to-ligand mole ratio of 2:3, which is in good agreement with the earlier reports of the single-crystal X-ray diffraction structure of $Dy_2L_3\cdot 5DMF$ [where L = 1,5-bis(1-phenyl-3-methyl-5-pyrazolone-4)-1,5-pentanedione].[18] On the other hand, **3** is ionic, and the $Tb^{3+}$ cation forms an anion by coordination to two molecules of $H_2SbBP$. The counterion is $Na^+$-dibenzo-18-crown-6. The IR spectra of the **1**−**3** exhibit a broad absorption in the 3000−3500 cm$^{-1}$ region, thus indicating the presence of water molecules in all three complexes. The carbonyl stretching frequency of free $H_2SbBP$ (1620 cm$^{-1}$) is shifted to lower energies upon complexation (1610 cm$^{-1}$ in **1**, 1618 cm$^{-1}$ in **2**, and 1613 cm$^{-1}$ in **3**). These data imply the coordination of the carbonyl

(18) Yang, L.; Yang, R. *J. Mol. Struct.* **1996**, *380*, 75–84.

**Scheme 3.** Synthesis Route to **3**

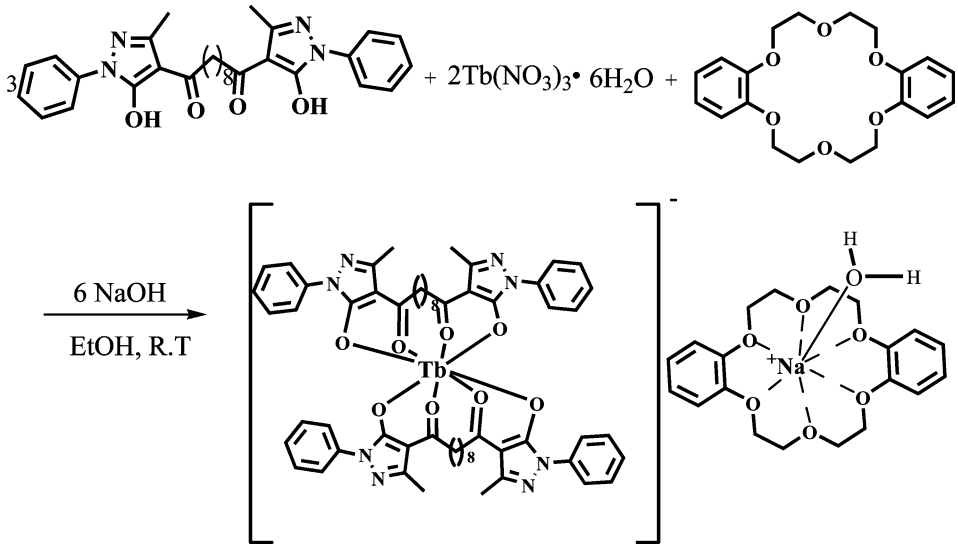


**Table 1.** Crystal data, Collection, and Structure Refinement Parameters for **3**

| parameters | **3** |
|---|---|
| empirical formula | $C_{80}H_{88}N_8NaO_{15}Tb$ |
| fw | 1583.49 |
| cryst syst | monoclinic |
| space group | *C*2/*c* |
| *T* | 153(2) K |
| *a* (Å) | 25.300(6) |
| *b* (Å) | 19.204(7) |
| *c* (Å) | 15.391(3) |
| α (deg) | 90° |
| *β* (deg) | 93.17(3)° |
| *γ* (deg) | 90° |
| *V* | 7467(4) Å$^3$ |
| *Z* | 4 |
| $\rho_{calcd}$ (g cm$^{-1}$) | 1.409 mg/m$^3$ |
| $\mu$ (mm$^{-1}$) | 1.025 mm$^{-1}$ |
| F(000) | 3280 |
| R1 | 0.0517 |
| wR2 | 0.0869 |
| R1 (all data) | 0.1340 |
| wR2 (all data) | 0.1081 |
| GOF | 0.95 |

**Table 2.** Selected Bond Lengths (Angstroms) and Angles (Degrees) for **3**

| **3** | lengths (Å) |
|---|---|
| O(1)−Na(1) | 2.586(4) |
| O(2)−Na(1) | 2.460(4) |
| O(3)−Na(1) | 2.574(4) |
| OW−Na(1) | 2.248(7) |
| Na(1)−O(2)#1 | 2.460(4) |
| Na(1)−O(3)#1 | 2.574(4) |
| Na(1)−O(1)#1 | 2.586(4) |
| O(7)−Tb(1) | 2.373(3) |
| O(8)−Tb(1) | 2.382(3) |
| O(9)−Tb(1) | 2.309(3) |
| O(10)−Tb(1) | 2.430(3) |
| Tb(1)−O(9)#2 | 2.309(3) |
| Tb(1)−O(7)#2 | 2.373(3) |
| Tb(1)−O(8)#2 | 2.382(3) |
| Tb(1)−O(10)#2 | 2.430(3) |
| Angles (Degrees) | |
| O(7)−Tb(1)−O(8) | 71.94 |
| O(9)−Tb(1)−O(10) | 71.69 |
| O(11)−Tb(1)−O(12) | 71.69 |
| O(13)−Tb(1)−O(14) | 71.94 |

oxygen takes place upon complex formation to the $Ln^{3+}$ ion. Moreover, the red shift observed for the characteristic C−O−C stretching frequencies of 1260 and 1120 cm$^{-1}$ for DB18C6 to 1253 and 1064 cm$^{-1}$ for **3** are indicative of $Na^+$ coordination.

The molecular structure of [Na(DB18C6)$H_2O$] [Tb(SbBP)$_2$] (**3**) was determined by single-crystal X-ray diffraction. Details of the crystal data and data collection parameters are given in Table 1, and selected bond lengths and bond angles are listed in Table 2. The complex crystallizes in the monoclinic space group *C*2/*c* with four [Na(DB18C6)$H_2O$] [Tb(SbBP)$_2$] molecules per unit cell ($Z = 4$). It is clear from the *ORTEP* diagram (Figure 2) that the solid state of **3** is ionic, and comprises an assembly of [Tb(SbBP)$_2$]$^-$ anions and [Na(DB18C6)$H_2O$]$^+$ cations. The $Tb^{3+}$ cation is surrounded by eight oxygen atoms furnished by two tetradentate bispyrazolone ligands. The formation of tetrakis ionic complexes of lanthanides with 4-acyl-5-pyrazolones are well documented.[19,20] However, the formation of ionic lanthanide complexes with 4-acylbis(pyrazolones) is not known. The coordination geometry around the $Tb^{3+}$ ion can be described best as distorted square antiprismatic. The Tb−O bond lengths range from 2.309−2.430 Å, with an average value of 2.37 Å, which is slightly larger compared to the Tb−O bond lengths (2.34 Å´) reported for the single-crystal X-ray structure of [Tb(PMPP)$_3$•$H_2O$]•EtOH (HPMPP = 1-phenyl-3-methyl-4-propionylpyrazol-5-one)[21] and Tb(Q$^{ETCP}$)$_3$($H_2O$) (2.36 Å) (Q$^{ETCP}$ = 1-phenyl-3-methyl-4-cyclopentenylcarbonyl-5-one).[22] This bond lengthening may be due to steric encumbrance by the acyl substituent.

The cationic species consists of a $Na^+$ cation surrounded by six oxygen atoms from the DB18C6 ligand and one oxygen atom from a water molecule, which adopts the apical

(19) Pettinari, C.; Marchetti, F.; Cingolani, A.; Drozdov, A.; Timokhin, I.; Troyanov, S. I.; Tsaryuk, V.; Zolin, V. *Inorg. Chim. Acta* **2004**, *375*, 4181–4190.
(20) Marchetti, F.; Pettinari, C.; Pettinari, R. *Coord. Chem. Rev.* **2005**, *249*, 2909–2945.

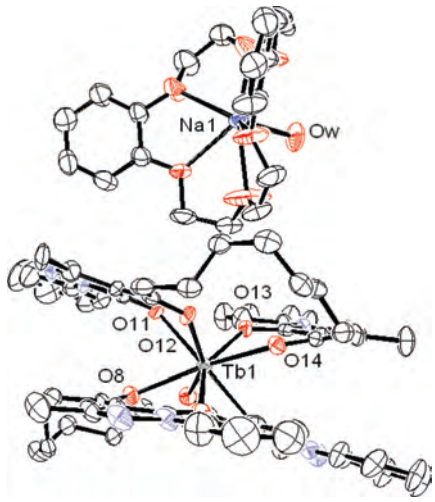


**Figure 2.** *ORTEP* diagram of $[Na(DB18C6)H_2O]$ $[Tb(SbBP)_2]$ with the thermal ellipsoids drawn at 30% probability level and the hydrogen atoms removed for clarity.

position of a distorted hexagonal pyramid. The latter structure is in good agreement with an earlier report.[23] However, most literature citations report a hexagonal-like coordination of the six oxygen atoms of the DB18C6 and the $Na^+$ ion.[24,25] The Na−O and C−C aliphatic distances of the cation are in good agreement with those already reported for sodium-crown ether complexes.[23–25] In the case of **3**, the water molecule plays a double role, namely (i) it stabilizes the $Na^+$ cation by coordination, and (ii) it serves as a bridge between the cation and anion by means of intermolecular hydrogen bonding with the oxygen and nitrogen atoms of the pyrazolone ligands.

**Intra- and Intermolecular Hydrogen Bonds and C−H−$\pi$ Stacking Interactions.** Supramolecular chemistry generally encompasses the chemistry of molecular recognition and self-assembly[26] and is mainly based on the noncovalent interactions such as metal coordination, hydrogen bonds, $\pi-\pi$ stacking, C−H−$\pi$, and van der Waals interactions.[27,28] Being reasonably strong and highly directional, hydrogen bonding interactions are widely used as structure-directing tools in supramolecular assembly for the generation of novel topological structures. In the present context, further analysis of the X-ray single-crystal structure of **3** reveals intramolecular hydrogen bonding between O9 of $H_2SbBP$ and C8 of DB18C6 through H8A with an O−H−C distance 2.306 Å and an angle of 163.35° (Figure S1 in the Supporting Information). The distance and angle between the donor and acceptor atoms found for **3** falls within the range reported for typical O−H−C hydrogen-bonding interactions.[29] Apart from the strong intramolecular hydrogen bonding interaction, a C−H−$\pi$ interaction is also observed in the case of **3**.

Specifically, this interaction is evident between C25 and C30 of $H_2SbBP$ and C2−H2 of DB18C6 as shown in Figure S2 in the Supporting Information. The relevant C−H−$\pi$ distances are 2.748 Å (152.97°) and 2.882 Å (168.70°). These two van der Waals interactions combine to give a unique 1D array, which involves alternate types of $Tb^{3+}$ and $Na^+$ coordination modes as illustrated in Figure 3.

Moreover, in addition to the interactions described above, intermolecular hydrogen bonding between the water oxygen atom of DB18C6 (OW) and the nitrogen atoms of $H_2SbBP$ (N4) is present in **3** as shown in Figure 4. The O−H−C distance 2.128 Å and the angle of 161.88° fall within the typical range of hydrogen bonding interactions.[27,28] These intra- and intermolecular hydrogen bonding and C−H−$\pi$ interactions combine to form an interesting molecular ladder, in which the alternate arrangement of metal coordination modes of $Tb^{3+}$ and $Na^+$ forms the strand and intermolecular hydrogen bonding connects the two 1D strands, thus forming the steps of the ladder as shown in Figure 5.

**UV−vis Spectra.** The UV−vis absorption spectra of the free ligand $H_2SbBP$ and the corresponding $Ln^{3+}$ complexes were measured in $CHCl_3$ solution ($c = 1 \times 10^{-5}$ M), and are shown in Figure 6. The maximum absorption bands at 291, 289, and 288 nm for **1**−**3**respectively are attributed to the singlet−singlet $^1\pi-\pi^*$ electronic transition of the aromatic rings that are present in the $\beta$-diketonate ligand. The absorption maxima are slightly red-shifted in **1**−**3** compared with the free ligand $H_2SbBP$ ($\lambda_{max}$= 286 nm), as a consequence of the enlargement of the conjugate structure of the ligand subsequent to coordination to the $Ln^{3+}$ ion. The shapes of the spectral bands for all three complexes are similar to that of the free ligand, suggesting that the coordination of the $Ln^{3+}$ ion does not have a significant influence on the $^1\pi-\pi^*$ transition. The molar absorption coefficient values ($\epsilon$) for **1** and **2** at $\lambda_{max}$ are $1.09 \times 10^4$ and $1.00 \times 10^4$ L mol$^{-1}$ cm$^{-1}$, respectively, which are about three times higher than that of $H_2SbBP$ ($3.72 \times 10^3$ L mol$^{-1}$ cm$^{-1}$ at 286 nm), indicating the presence of three $H_2SbBP$ ligand molecules in each of the three complexes. In the case of **3**, the $\epsilon$ value ($7.338 \times 10^3$ L mol$^{-1}$ cm$^{-1}$) is found to be twice that of free ligand, which indicates the involvement of two $H_2SbBP$ ligands.

**Photophysical Properties of the Complexes.** The normalized steady-state excitation and emission spectra of terbium complexes **1** and **3** at room temperature (in the solid state) are depicted in Figures 7 and 8, respectively. The excitation spectra of $Tb^{3+}$ complexes **1** and **3** monitored

(21) Drozdov, A.; Vertlib, V.; Timokhin, I.; Troyanov, S.; Pettinari, C.; Marchetti, F. *Russ. J. Coord. Chem.* **2002**, *28*, 259–263.
(22) Pettinari, C.; Pettinari, R.; Marchetti, F.; Drozdov, A.; Timokhin, I.; Semenov, S.; Troyanov, S. I. *Inorg. Chem. Commun.* **2003**, *6*, 1423–1425.
(23) Dapporto, P.; Paoli, P.; Matijasic, I.; Tusek-Bozic, L. *Inorg. Chim. Acta* **1998**, *282*, 76–81.
(24) Dreissig, W.; Dauter, Z.; Cygan, A.; Biemat, J. F. *Inorg. Chim. Acta* **1985**, *96*, 21–27.
(25) Mashiko, T.; Reed, C. A.; Haller, K. J.; Scheidt, W. R. *Inorg. Chem.* **1984**, *23*, 3192–3196.
(26) Hu, M.; Wang, X.; Jiang, Y.; Li, S. *Inorg. Chem. Commun.* **2008**, *11*, 85–88.
(27) Atwood, J. L.; Davies, J. E. D.; MacNicol, D. D.; Vogtle, F. *Comprehensive Supramolecular Chemistry*; Pergamon: New York, 1996.
(28) (a) Gokel, G. W. *Crown Ethers and Cryptands, Royal Society of Chemistry*; Cambridge, 1994. (b) Gokel, G. W. *Comprehensive Supramolecular Chemistry, Molecular Recognition: Receptors for Cationic Guest*, Vol. *1*; Pergamon: New York, 1996. (c) Nishio, M. Hirota, M. Umezawa Y. *The CH-π Interaction*; Wiley VCH: New York, 1998.
(29) Roesky, H. W.; Andruh, M. *Coord. Chem. Rev.* **2003**, *236*, 91–119.

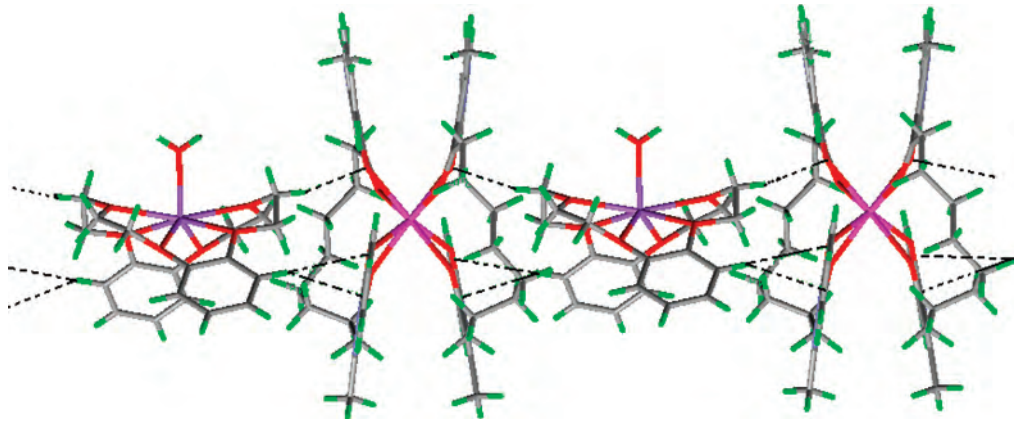

**Figure 3.** 1D array consisting alternate arrangements of $Tb^{3+}$ and $Na^{+}$ coordination modes.

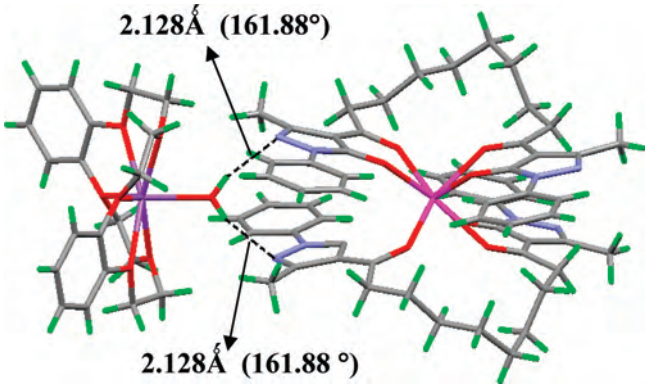


**Figure 4.** Intermolecular hydrogen bond present in **3** between water oxygen atom of DB18C6 (OW) and nitrogen atoms of $H_2SbBP$ (N4) (shown with broken lines).

around the peak of the intense $^5D_4 \rightarrow {}^7F_5$ transition of the $Tb^{3+}$ ion exhibit a broad band between 245 and 400 nm with a maximum at approximately 338 nm, which can be assigned to the $^1\pi-\pi^*$ electronic transition of the $H_2SbBP$. The absence of any absorption bands due to the f−f transition of the $Tb^{3+}$ cation proves that luminescence sensitization via excitation of the ligand is more effective than direct excitation of the $Tb^{3+}$ ion.

The room-temperature normalized emission spectra of terbium complexes **1** and **3** exhibit the characteristic emission bands for $Tb^{3+}$ ($\lambda_{ex} = 338$ nm) centered at 490, 545, 585, and 620 nm, which result from deactivation of the $^5D_4$ excited state to the corresponding ground state $^7F_J$ ($J = 6, 5, 4, 3$) of the $Tb^{3+}$ ion. The most intense emission is centered at 545 nm and corresponds to the transition $^5D_4 \rightarrow {}^7F_5$.[30] No emission bands from $H_2SbBP$ or DB18C6 or LMCT are observed in these complexes, thus indicating the efficient energy transfer from the corresponding ligands to the central $Tb^{3+}$ ion.

The overall quantum yield ($\Phi_{overall}$) for a lanthanide complex treats the system as a black box in which the internal process is not considered explicitly. Given that the complex absorbs a photon (i.e., the antenna is excited), the overall quantum yield can be defined as follows:[31]

$$\Phi_{overall} = \Phi_{transfer}\Phi_{Ln} \quad (2)$$

Here, $\Phi_{transfer}$ represents the efficiency of energy transfer from the ligand to the $Ln^{3+}$ ion, and $\Phi_{Ln}$ represents the intrinsic quantum yield of the $Tb^{3+}$ ion. The overall quantum yield ($\Phi_{overall}$) for terbium complexes **1** and **3** calculated according to the procedure described by Bril et al.[15] are 4.82 ± 0.01% and 18.13 ± 0.82%, respectively. The creation of $Ln^{3+}$ complexes with higher quantum yields is linked directly to suppression of radiationless transitions caused by vibrational excitations in the surrounding media.[32,33] The lower quantum yield value obtained in the case of **1** may be due to the presence of solvent molecules in the coordination sphere, which effectively quench the luminescence of the $Tb^{3+}$ ion. Furthermore, it may also be a consequence of energy transfer between the $Tb^{3+}$ ions themselves which is a well-recognized nonradiative process, for homodinuclear lanthanide complexes.[34] On the other hand, the quantum yield of **3** is approximately three times higher than that of **1** due to the absence of nonradiative decay channels in the coordination sphere of the $Tb^{3+}$ cation. Additionally, the DB18C6 present in the crystal lattice of **3** may also cause energy transfer to the neighboring $H_2SbBP$ ligand. Following this, the $H_2SbBP$ ligand subsequently transfers energy to the $Tb^{3+}$ cation via the usual triplet pathway, thus explaining the increased luminescence intensity in the present study.

The $^5D_4$ lifetime values ($\tau_{obs}$) at room temperature were determined from the luminescent decay profiles for **1** and **3** by fitting the data with a monoexponential curve, thereby indicating the presence of a single-chemical environment around the emitting $Tb^{3+}$ ion. The lifetime values for **1** and

(30) (a) Carnall, W. T. In *Handbook on the Physics and Chemistry of Rare Earths*; Gschneidner, K. A., Eyring, L., Eds.; Elsevier: Amsterdam, The Netherlands, 1987; Vol. *3*, Chapter 24, pp 171−208. (b) Dieke, G. H. *Spectra and Energy levels of Rare Earth Ions in Crystals*; Interscience: New York, 1968.

(31) (a) Xiao, M.; Selvin, P. R. *J. Am. Chem. Soc.* **2001**, *123*, 7067–7073. (b) Comby, S.; Imbert, D.; Anne-Sophie, C.; Bünzli, J.-C. G.; Charvonniere, L. J.; Ziessel, R. F. *Inorg. Chem.* **2004**, *43*, 7369–7379. (c) Quici, S.; Cavazzini, M.; Marzanni, G.; Accorsi, G.; Armaroli, N.; Ventura, B.; Barigelletti, F. *Inorg. Chem.* **2005**, *44*, 529–537.

(32) (a) Peng, C.; Zhang, H.; Yu, J.; Meng, Q.; Fu, L.; Li, H.; Sun, L.; Guo, X. *J. Phys. Chem. B* **2005**, *109*, 15278–15287. (b) Wada, Y.; Ohkubo, T.; Ryo, M.; Nakarawa, T.; Hasegawa, Y.; Yanagida, S. *J. Am. Chem. Soc.* **2000**, *122*, 8583–8584.

(33) Fu, L.; Sa' Ferreira, R. A.; Silva, N. J. O.; Fernandes, J. A.; Ribeiro-Claro, P.; Goncüalves, I. S.; de Zea Bermudez, V.; Carlos, L. D. *J. Mater. Chem.* **2005**, *15*, 3117–3125.

(34) Li, Q.; Li, T.; Wu, J. *J. Phys. Chem. B* **2001**, *105*, 12293–12296.

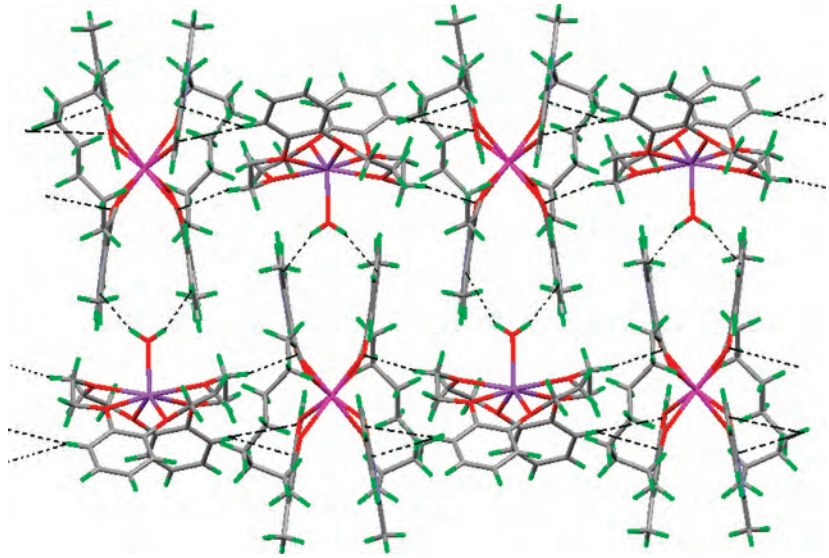

**Figure 5.** Molecular ladder of **3** involving intra- and intermolecular hydrogen bonding and C−H−$\pi$ interactions.

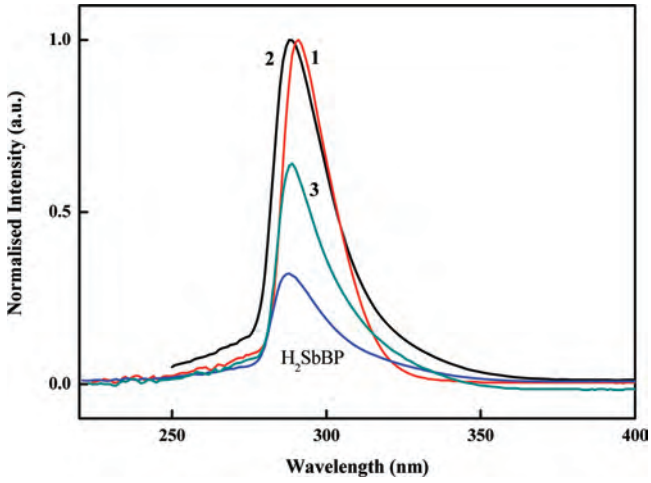


**Figure 6.** UV−vis spectra $H_2SbBP$, $Tb_2(SbBP)_3 \cdot 2H_2O$ (**1**), $Gd_2(SbBP)_3 \cdot 2H_2O$ (**2**), and $[Na(DB18C6)H_2O][Tb(SbBP)_2]$ (**3**) in $CHCl_3$ ($c = 1 \times 10^{-5}$ M).

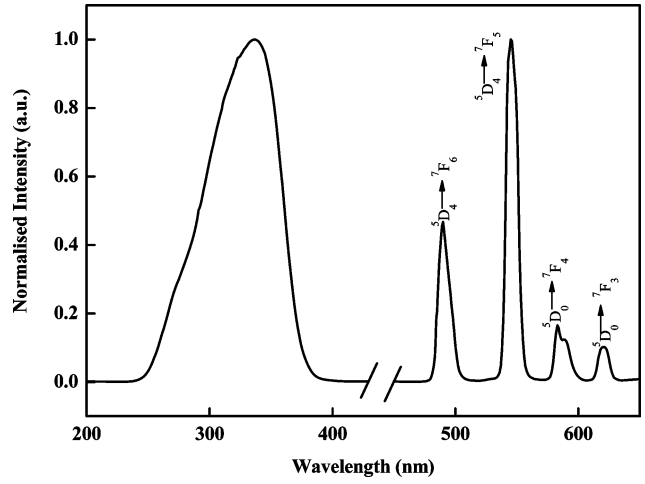


**Figure 7.** Room-temperature (300 K) excitation and emission spectra for **1** ($\lambda_{ex} = 336$ nm) with emissions monitored around 545 nm.

**3** were found to be 1.11 ± 0.01 and 2.82 ± 0.02 ms, respectively. Some typical decay profiles for complexes are exhibited in Figure 9. The somewhat shorter lifetime

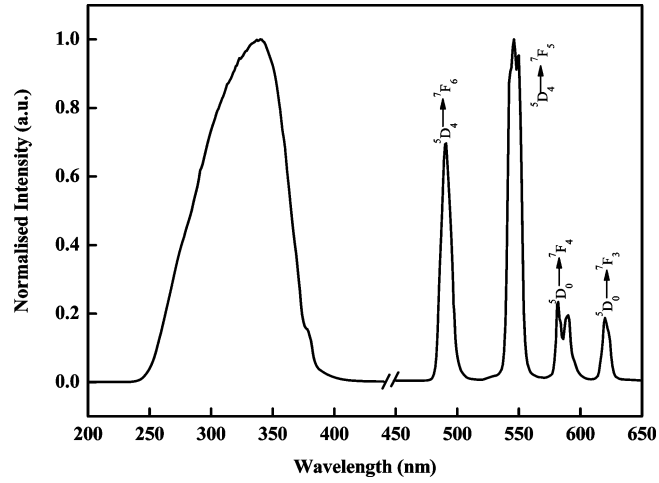


**Figure 8.** Room-temperature (300 K) excitation and emission spectra for **3** ($\lambda_{ex} = 339$ nm) with emissions monitored at 545 nm.

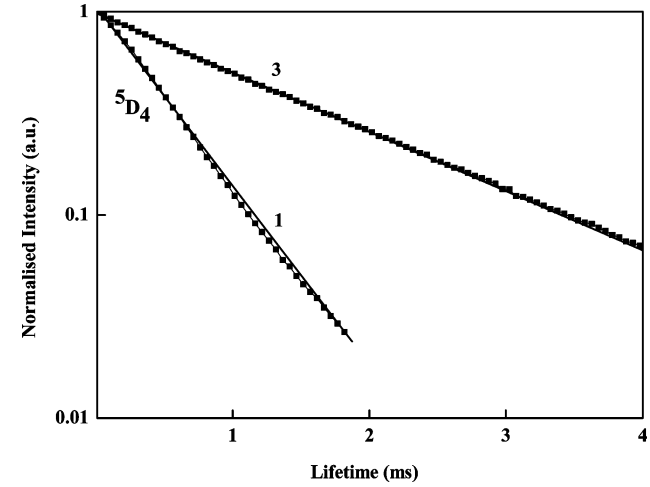


**Figure 9.** Luminescence decay profiles of **1** ($\lambda_{ex} = 336$ nm) and **3** ($\lambda_{ex} = 339$ nm) and monitored around 545 nm.

observed for **1** may be due to the presence of dominant nonradiative decay channels that are associated with vibronic coupling due to the presence of solvent molecules. This effect has been well documented for several hydrated terbium

$\beta$-diketonate complexes.[12d] However, a longer lifetime value has been observed in the case of **3** due to the absence of nonradiative decay pathways.

**Energy Transfer between the Ligand and $Tb^{3+}$.** In general, the sensitization pathway in luminescent terbium complexes consists of excitation of the coordinated ligands into their excited states, subsequently intersystem crossing of the ligands to their triplet states and energy transfer from the triplet state of the ligand to the $^5D_J$ manifold of the $Tb^{3+}$ ion. This is followed by internal conversion to the emitting $^5D_4$ state, and finally the $Tb^{3+}$ ion emits radiation. Therefore, the energy-level match between the triplet states of the ligands to the $^5D_4$ state of the $Tb^{3+}$ cation is one of the key factors that govern the luminescence properties of terbium complexes. The phosphorescence spectra of the complexes $Gd_2(SbBP)_3(H_2O)_2$ and $Gd(DB18C6)_2(NO_3)_3(H_2O)_2$ (Figure S3 in the Supporting Information) were measured for the triplet energy level data of the ligands. On the basis of the phosphorescence spectra, the triplet energy levels of $Gd_2(SbBP)_3(H_2O)_2$ and $Gd(DB18C6)_2(NO_3)_3(H_2O)_2$ correspond to their lower emission edge wavelengths and appear at 23 201 $cm^{-1}$ (431 nm) and 24 154 $cm^{-1}$ (414 nm), respectively. Because the lowest excited energy level of the $Gd^{3+}$ cation ($^6P_{7/2}$) is too high to accept energy from the ligands, the data obtained from the phosphorescence spectra actually reveal the triplet energy levels ($^3\pi\pi^*$) of $H_2SbBP$ and DB18C6 in the $Tb^{3+}$ complexes. The singlet energy levels ($^1\pi\pi^*$) of $H_2SbBP$ and DB18C6 can be estimated by referencing their higher absorption edges, which appear at 32 839 $cm^{-1}$ (304 nm) and 34 722 $cm^{-1}$ (288 nm), respectively.

It is well-known that in organolanthanide complexes neutral ligands often play a role in terms of absorbing and transporting energy to other ligands or to the central metal ion.[35] It is clear from Figure S3 in the Supporting Information that there is a large area of overlap between the room-temperature emission spectrum of DB18C6 and the phosphorescence spectrum of $Gd_2(SbBP)_3(H_2O)_2$, hence any DB18C6 present in the crystal lattice of **3** can efficiently transfer its absorbed energy to the triplet state of the $H_2SbBP$. Furthermore, the DB18C6 ligand can also undergo intersystem crossing. The overlap of the low-temperature phosphorescence spectra of complexes $Gd_2(SbBP)_3(H_2O)_2$ and $Gd(DB18C6)_2(NO_3)_3(H_2O)_2$ is suggestive of the possibility of energy transfer from the triplet state of DB18C6 to the triplet state of the $H_2SbBP$. According to Reinhoudt's empirical rule, the intersystem crossing will be effective when $\Delta E = {}^1\pi\pi^* - {}^3\pi\pi^*$ and is at least 5000 $cm^{-1}$.[36] The gaps between the $^1\pi\pi^*$ and $^3\pi\pi^*$ states of $H_2SbBP$ and DB18C6 ($\Delta E = {}^1\pi\pi^* - {}^3\pi\pi^* = 9638$ $cm^{-1}$ and 10 568 $cm^{-1}$, respectively) are favorable for a relatively efficient intersystem crossing process in the present complexes. Latva's empirical rule[37] states that an optimal ligand-to-metal energy transfer process for $Tb^{3+}$ requires $2500 < \Delta E\ (^3\pi\pi^* - {}^5D_J) < 4500$ $cm^{-1}$. The triplet energy levels of $H_2SbBP$ (23 201 $cm^{-1}$) and DB18C6 (24 514 $cm^{-1}$) appear at appreciably higher energy than the $^5D_4$ level of $Tb^{3+}$ (20 400 $cm^{-1}$), and hence effective energy transfer can occur in the complexes described herein. A schematic energy-level diagram based on the foregoing is presented in Figure 10.

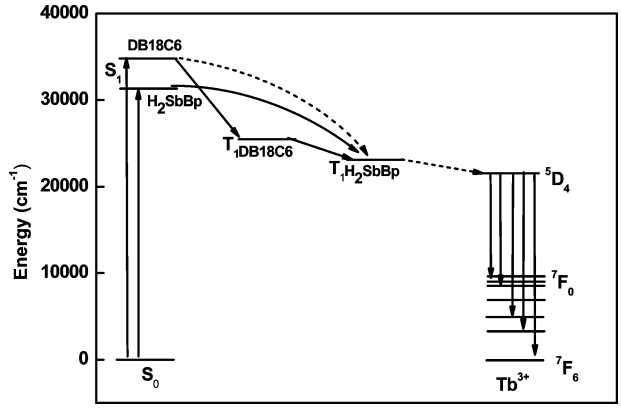


**Figure 10.** Schematic energy-level diagram and the energy transfer process. $S_1$, singlet excited state; $T_1$, triplet excited state.

## Conclusion

Three new $Ln^{3+}$ complexes (**1**−**3**) based on coordination to a novel heterocyclic $\beta$-diketone, 4-sebacoylbis(1-phenyl-3-methyl-5-pyrazolone have been synthesized. One such complex (**3**) has been structurally characterized by single-crystal X-ray diffraction. The X-ray crystal structure of **3** confirms the formation of the ionic complex $[Na(DB18C6)H_2O]$ $[Tb(SbBP)_2]$. The analysis of single-crystal data further reveals the formation of an interesting 1D molecular ladder structure, which is held together by C−H−$\pi$, intra-, and intermolecular hydrogen bonding. The $Tb^{3+}$ complexes of 4-sebacoylbis(1-phenyl-3-methyl-5-pyrazolonate), **1** and **3**, exhibit bright-green luminescence with quantum yield values of 4.82 ± 0.01% and 18.13 ± 0.82%, and $^5D_4$ lifetime values 1.11 ± 0.01 and 2.82 ± 0.02 ms, respectively. The sensitization mechanism for the luminescent $Tb^{3+}$-bis-4-acyl-pyrazolonate complexes involves the usual triplet pathway, in which energy absorbed by the ligand is efficiently transferred to the emitting level of central metal ion. Because of the large overlap of the emission bands of the macrocyclic ligand, with those of the heterocyclic $\beta$-diketonate, the secondary ligand also successfully transfers absorbed energy to the metal center through the triplet state of the primary ligand, which is present in the coordination sphere of the $Tb^{3+}$ cation. This effect may be responsible for the significant improvement of luminescent efficiency observed in the case of ionic complex **3**. The high luminescence efficiencies exhibited by the present $Tb^{3+}$ complexes herald promising applications in many photonic devices.

**Acknowledgment.** The authors would like to acknowledge the financial support from Defence Research and Development Organization and Council of Scientific and Industrial Research (NWP0023), New Delhi, India. The authors also wish to thank

(35) Xu, H.; Wang, L.; Zhu, X.; Yin, K.; Zhong, G.; Hou, X.; Huang, W. *J. Phys. Chem. B* **2006**, *110*, 3023–3029.
(36) Steemers, F. J.; Verboom, W.; Reinhoudt, D. N.; vander Tol, E. B.; Verhoeven, J. W. *J. Am. Chem. Soc.* **1995**, *117*, 9408–9414.
(37) Latva, M.; Takalo, H.; Mukkala, V. M.; Matachescu, C.; Rodriguez-Ubis, J. C.; Kankare, J. *J. Lumin.* **1997**, *75*, 149–169.

Prof. T. K. Chandrashekar, Director National Institute for Interdisciplinary Science and Technology, Trivandrum, India, for his constant encouragement and valuable discussions. A.H.C. thanks the Robert A. Welch Foundation (F-0003) for financial support.

**Supporting Information Available:** Intramolecular hydrogen bonding, C−H−$\pi$ stacking interactions present in **3** and phosphorescence spectra of the ligands. This material is available free of charge via the Internet at http://pubs.acs.org. X-ray crystallographic information files can be obtained free of charge via www.ccdc.cam.ac.uk/consts/retrieving.html (or from CCDC, 12 Union Road, Cambridge CB2 1EZ, U.K.; fax +44 1223 336033; e-mail deposit@ccdc.cam.ac.uk). CCDC 679579 for **3** in this article.

IC800615Y